Simulation of HFCT PD Detection in MV Bus Bar Chamber

Mijodrag Miljanovic
The Institute of Energy and Environment,
Dept. of Electronic & Electrical Engineering
University of Strathclyde
Glasgow, UK
mijodrag.miljanovic@strath.ac.uk

Martin Kearns
EDF (UK)
East Kilbride, UK
martin.kearns@edf-energy.com

Brian G Stewart
The Institute of Energy and Environment,
Dept. of Electronic & Electrical Engineering
University of Strathclyde
Glasgow, UK
brian.stewart.100@strath.ac.uk

***Abstract*—A simulation investigation is conducted for high frequency current transformers (HFCT) partial discharge (PD) detection on a grounding conductor in a medium voltage (MV) switchgear compartment. A three-dimensional (3-D) bus bar chamber of an air insulated MV metal clad switchgear including PD sources and grounding position is developed using Comsol Multiphysics. The PD sources are placed at different locations in the chamber and the sensitivity of the HFCT signal is investigated depending of different position of the bus bar chamber grounding. The current induced by PD in the grounding conductor is provided as input to the HFCT sensor. Throughout the simulation it can be seen that there is an influence on the sensitivity of the HFCT signal depending on the grounding position. The analysis helps also to inform the nature of HFCT signals related to different PD locations and grounding wire positions which will help to refine and understand better HFCT measurements for condition monitoring within such systems.**

Keywords—bus bar chamber, partial discharge, high frequency current transformer, finite element method, grounding conductor

I. Introduction

The monitoring of partial discharge (PD) activity within high voltage (HV) and medium voltage (MV) equipment can help to avoid insulation failures in electrical power systems. Generally, there are two different methods employed in PD detection. The first is the conventional approach that is mainly used for acceptance tests and is described by the standards EN 60270:2001, IEEE Std 1291-1993 and IEC Std C57.113-2010. The second, is the non-conventional and non-intrusive approach, which is common for onsite PD monitoring and is covered by IEC technical specification PD IEC/TS 62478:2016. This technical standard specifies different non-intrusive methods and among which is the application of high frequency current transformers (HFCTs).

A significant quantity of research has previously been conducted regarding the design and application of HFCT sensors for PD measurement. Estimation of HFCT equivalent circuit electrical parameters, either through simulation [1] or through experimental work [2] has also been a focus of research. However, for MV switchgear little work has been presented that investigates HFCT sensor response and sensitivity when both the position of any PD and the position of the associated switchgear chamber grounding conductor is changed [3].

The aim of this work is therefore to analyse the sensitivity of the HFCT signal as a function of different PD source locations and grounding positions within a bus bar chamber. In this paper, the simulation study response of an HFCT sensor is studied when PD occurs at variable locations within a switchgear chamber and also when the grounding conductor is connected to different positions along the compartment. The analysis will help inform the nature of HFCT response signals related to different PD locations and to refine HFCT measurement techniques for switchgear evaluation. The ultimate aim of such an analysis would be to further inform the understanding of how an improved online non-intrusive PD detection and condition monitoring system for MV bus bar chambers could be deployed.

II. Simulation Model

A. Bus bar compartment model

A three-dimensional (3-D) finite element model (FEM) of a single MV switchgear bus bar chamber is created in Comsol software, Fig. 1(a). The enclosure of the chamber is modelled as 3 mm solid aluminium. The bus bar supports are made from epoxy resin and the conductors are modelled as bare copper conductors. The grounding conductor can be placed at different positions on the bottom wall and is shaped as 50 mm² cross section copper wire. The PD sources are placed at the bus bar supports. Since one open-ended compartment is modelled, the electromagnetic (EM) signals also propagate out the chamber.

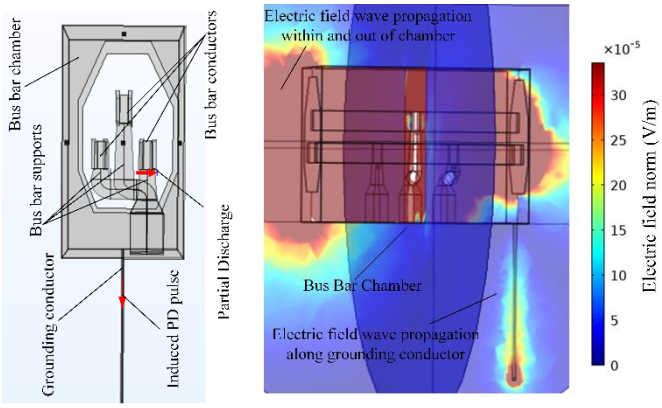

(a) 3-D Model (b) EM Wave Propagation

Fig. 1. (a) 3-D model of MV switchgear bus bar chamber, and (b) EM wave propagtion through the compartment and along the grounding conductor.

This work was funded by the EDF UK

B. *High frequency current transformer circuitry*

The HFCT circuit was implemented in the same 3-D model environment. The equivalent electrical circuit according to [4] of the used sensor can be seen in Fig. 2. An explanation of the different electrical elements and their values are listed in Table I. The numbered points in Fig. 2 within the circuit indicate the circuit nodes which define the equivalent circuit of the HFCT sensor and the measuring elements. The bandwidth of the HFCT sensor was also analyzed. In Fig. 3 the frequency band of the sensor is displayed when the circuit is loaded with a resistor of 50 Ohms. It can be seen that the frequency band of the HFCT circuit lays between 300 kHz and 10 MHz, which is a common value for such sensors. Using a so-called lumped port in Comsol, the interconnection between the 3-D model and the HFCT circuit is established. The induced PD current in the grounding conductor is provided through this port to the HFCT circuit. Finally, the current generates the PD voltage that is measured at the end of the circuit.

C. *Sensitivity investigation*

An investigation of the HFCT sensitivity is performed by moving the grounding conductor to four different positions along the bus bar chamber. The possible grounding positions are indicated through points 1 to 4 in Fig. 4, where the top view of the compartment is shown. As can be seen, grounding points 1 and 3 are at the left- and right-hand sides of the compartment, respectively. Grounding positions 2 and 4 are at the top and bottom sides of the compartment, when looking from the top view perspective. The positions of PD sources are indicated by the arrows PDL1, PDL2 and PDL3 in Fig. 4. They are placed on the bus bar supports of the particular phase. In addition, the arrows point in the direction that the PD current pulse takes place. In this investigation all of the PD sources possess the same current pulse direction. The orientation of each of the PD sources could be also changed, but this is not considered in this work.

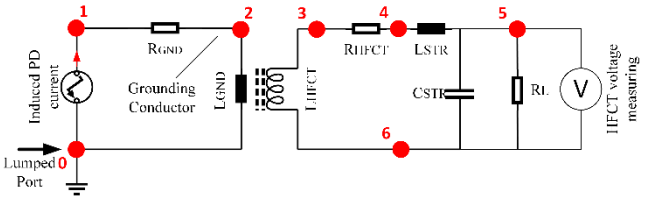

Fig. 2. Equivalent electrical circuit of HFCT and measuring elements

TABLE I. HFCT CIRCUIT PARAMETERS

Parameter name	Parameters of the HFCT circuit	
	Sign	***Value***
Grounding cond. resistance	R_{GND}	2 Ohms
Gorunding cond. inductance	L_{GND}	1uH
HFCT magn. inductance	L_{HFCT}	100uH
HFCT circuit resistance	R_{HFCT}	2 Ohms
HFCT stray inductance	L_{STR}	0.7uH
HFCT stray capacitance	C_{STR}	200 pF
Load resistance	R_L	50 Ohms

This work was funded by the EDF UK

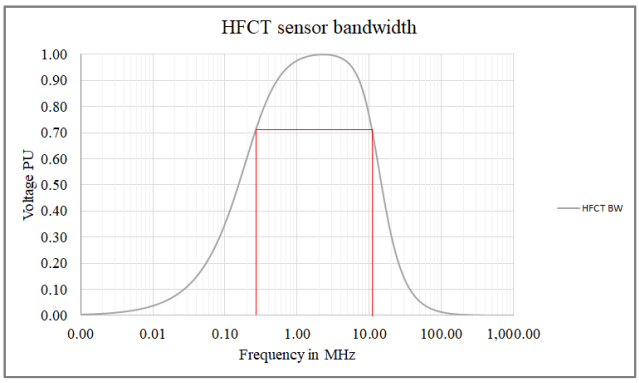

Fig. 3. HFCT sensor bandwidth with 50 Ohms load resistance

D. *PD source*

The PD source is implemented as a rectangular lumped port in the FEM environment, with a height of 20 mm and a width of 15 mm. The lumped port represents the surface discharge current density in the z-direction along the particular bus bar support. The locations where the PD occurs in the model is marked by the arrows in Fig. 4. The PD current pulse $i_{PD}(t)$ is implemented through a normalized Gaussian function according to [5], described through Eq. (1).

$$i_{PD}(t) = I_0 * e^{-[\frac{(t-t1)^2}{2*\tau^2}]} \qquad (1)$$

The peak current is represented by I_0, which is set for simplicity to 1A. The time of occurrence of the PD peak current is determined by the term t1, which is set to 5ns. The term τ represents the pulse width parameter, which is set to 1 ns in this investigation. Using the stated variables above, different rise and fall times of the PD sources may be implemented, thus, enabling different PD pulse shapes to be emulated in the simulation. According to the applied parameters above, the rise and fall times of the induced PD current in the grounding conductor are in the range of 10 ns.

E. *Simulation Configuraiton*

The simulation is conducted in the time domain using the Comsol EM Wave Transient node. The simulations are conducted using the PARADISO solver with Generalized alpha time step. The simulation time step is set to 1 ps with simulation duration set up to be 500 ns. In a first investigation step, the sensitivity of the HFCT sensor at the four different grounding positions is performed for each of the three separate PD sources. Secondly, the sensitivity and the signals are shown for the case of when there is no termination resistance at the output of the HFCT circuit.

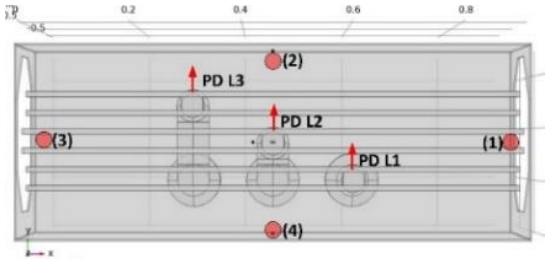

Fig. 4. Top view of the bus bar compartment and the grounding conductor location (dots) and PD position (arows).

III. Simulation Results

A. HFCT sensitivity at different grounding positions

The simulated HFCT sensitivity responses are shown in Figs. 5 to 8 for the different grounding positions and PD locations. The per-unit (pu) method is used to express the voltage levels in the graphs for the sake of a better comparison between the measurements. The reference voltage for the pu calculation is in relation to the highest amplitude detected when no 50 Ohms termination is applied.

In Fig. 5 the HFCT signals are displayed for the 3 different PD source locations for the case when the chamber is earthed at position 1. Comparing the graphs, it can be seen that the measured signal for PDL1 possesses the highest amplitude. This is due to the fact that the source PDL1 is closer to the particular measuring ground point. Interestingly, the amplitude of PDL2 seems to be lower compared to the amplitude of PDL3 although this PD source is closer to the measuring point. This might be due to the complexity of the propagation path of the EM wave and the resulting induction of the PD current in the grounding wire. In Fig. 6 the HFCT signal is shown when measuring on grounding position 2. The highest detected signal is again for source PDL1. Interestingly, the amplitude of the measured signal for PDL2 is lower comparing to PDL3, even if closer to the measuring point. The reason could be due to obstructions from the higher position of the bus bar support and the particular PD in the compartment compared to the other two PD sources. In Fig. 7 the HFCT signals at grounding position 3 are displayed for the three PD sources. It can be seen that the amplitude from PDL3 is the highest. This is likely due to the vicinity of the PDL3 source to the measuring point compared to other two PD sources. In Fig. 8 the HFCT signals are shown for grounding position 4 of the compartment. Compared to the other two PD sources, PDL1 possesses the highest amplitude. The amplitude of PDL3 is higher than PDL2. Even though PDL2 seems to be closer to the measuring point it has the lowest amplitude. The reason for this is again likely due to the position of the PD sources in the compartment producing different EM propagation environments to the chamber walls from the PD locations.

Generally, it can be said that the highest peak measured is at the grounding position 1, when PDL1 is active. In addition to that, the highest sensitivity for PDL2 and PDL3 is located at grounding position 3. These two grounding places appear to be most appropriate for HFCT measurements for the scenarios considered. Clearly, a more comprehensive set of investigations are required for different PD locations and PD pulse widths situations.

B. Influence of the HFCT termination

Another interesting aspect investigated in the current work, is the influence of the 50 Ohms termination of the HFCT circuit on the sensitivity. In Figs. 9 and 10, the detected PD signals are shown without a 50 Ohms circuit termination for grounding points 1 and 3. Comparing these waveforms to the signals with the 50 Ohms termination in Fig. 5 and Fig. 7, the damping effect of the termination resistance can be clearly recognized. Without the 50 Ohm termination there is significant ringing of the detected signals. Obviously, the termination resistance as expected changes the waveforms of the detected signals.

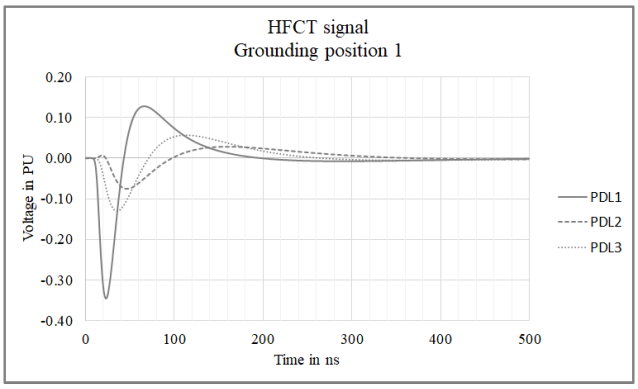

Fig. 5. HFCT signal measured at grounding position (1)

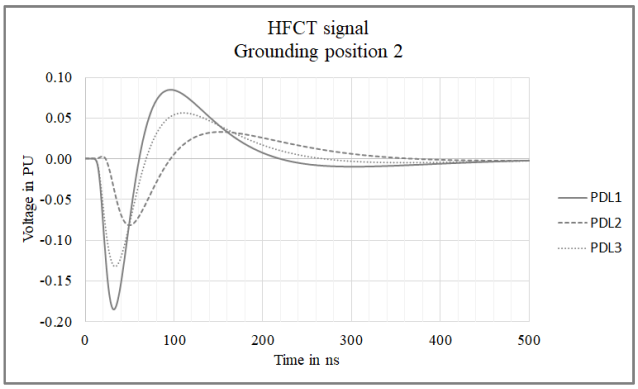

Fig. 6. HFCT signal signal measured at grounding position (2)

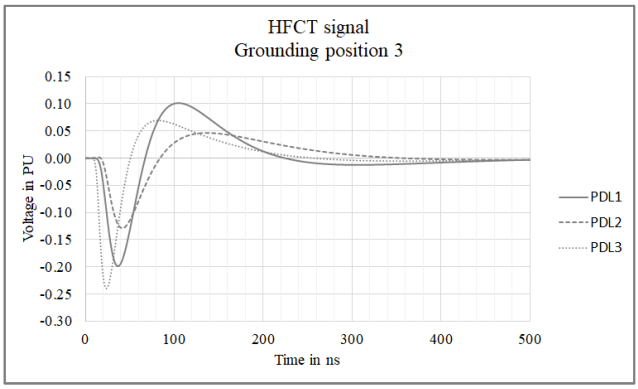

Fig. 7. HFCT signal measured at grounding position (3)

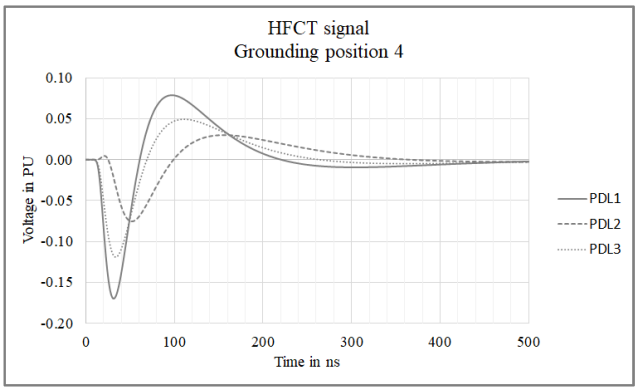

Fig. 8. HFCT signal signal measured at grounding position (4)

When comparing the cases with and without termination, for HFCT termination, the highest amplitude appears at grounding position 1, see Fig. 5. In contrast with no termination resistor, the highest amplitude is measured at grounding position 3, as shown in Fig. 10. In the particular case when looking at the time arrival of the signal in Fig. 10, PDL3 is closer to the measuring point, despite its amplitude being lower compared to PDL1. The influence of the EM wave propagation and the internal structure of the chamber clearly plays an important role in the induction of the HFCT voltages and the sensitivity. In summary, when conducting measurements, the termination resistance will influence where the highest signal is going to be detected. For grounding position 3, for both terminated and unterminated cases highest detected waveform signals for the PD sources are consistent.

C. *Frequency range of the HFCT signals*

Despite the termination resistance, it should be noted that the general period (not the initial rise time) of the detected HFCT waveform response remains similar. This can be seen when comparing the periods of the first wave of the measured signals in the Fig. 5 to Fig. 8 with the signal periods in Figs. 9 and 10. It can be seen that the period of each detected PD signal is about 200 ns. That corresponds to the frequency of around 5 MHz, which is in the approximate HFCT bandwidth shown in Fig. 3.

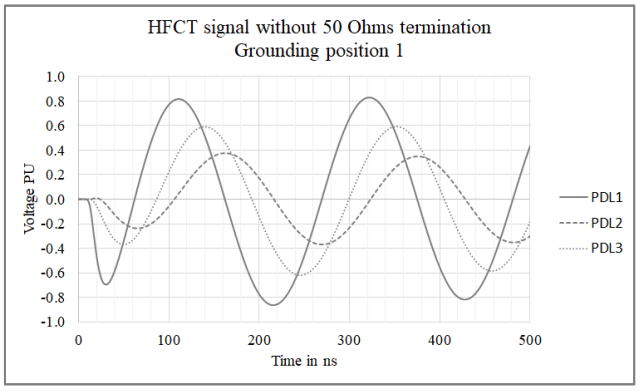

Fig. 9. HFCT signal measured at grounding position (1) without HFCT termination resistor

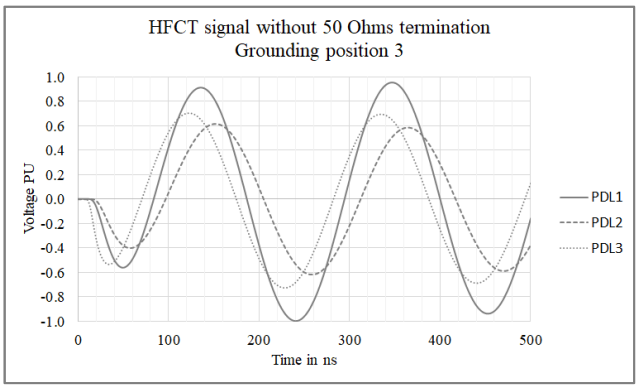

Fig. 10. HFCT signal measured at grounding position (3) without HFCT termination resistor

IV. Conclusions

Throughout simulation it is shown that the sensitivity of an HFCT sensor location for PD detection can be changed or increased at different grounding positions of the bus bar chamber. Some grounding positions for PD detection using the HFCT provide increased amplitudes compared to other positions. In addition, due to propagation path changes the HFCT location may introduce some signal delay and different initial signal rise times. The structure of the compartment clearly influences the EM wave propagation from the PD sources. Thus, depending on the PD signal location and the HFCT location the HFCT waveforms will produce different waveform amplitudes and rise times. In this particular work the same orientation of the PD sources was chosen for the investigation. For the grounding positions considered it has been shown that the grounding positions 1 and 3 would be most effective for PD detection for HFCT detection in the considered bus bar chamber.

As expected, the measuring termination of an HFCT circuit changes the damping characteristics of the signals. The signal amplitudes without termination appear with higher ringing effect and lower damping. What remains similar for both terminated and unterminated cases is the arrival time of the signals and the general waveform frequency response of the HFCT.

Determining optimum HFCT grounding positions for multiple types of internal PD locations still requires investigation with the purpose of understanding how best to determine the precise source location based on HFCT response. Future work will be focused on investigations with different PD source locations, different PD pulse widths, alternative grounding positions and different HFCT designs. As can be seen, the internal structure of the bus bar chamber also plays an important role on the EM wave propagation. Therefore the induced HFCT voltages in case of different structures may also be investigated.

References

[1] C. Zachariades, R.Shuttleworth, R. Giussani, R. MacKinlay, “Optimization of a High Frequency Current Transformer sensor for Partial Discharge Detection using Finite Element Analysis,” IEEE Sensors Journal, vol. 16, no. 20, pp. 7526-7533, Oct. 15, 2016.

[2] J.V. Klüss, A-P. Elg, C. Wingqvist, “High-Frequency Current Transformer Design and Implementation Considerations for Wideband Partial Discharge Applications,” IEEE Transactions and Measurement, vol. 70, pp. 1-9, January, 2021.

[3] Wenbo Fan et al., “Comparison Study of Partial Discharge Detection Methods for Switchgears,” 2016 International Conference on Condition Monitoring and Diagnostics (CMD), pp. 319-323, Sept., 2016.

[4] H. Hu, W.H. Siew, M.D. Judd, X. Peng, “Transfer Function Characterization for HFCTs Used in Partial Discharge Detection,” IEEE Transactions on Dielectrics and Electrical Insulation, vol. 24, no.2, pp. 1088-1096, April., 2017.

[5] T. Zhao, M.D. Judd, B.G. Stewart, “Attenuation Characteristics and Time Delay of PD Electromagnetic Wave Propagation in GIS Systems,” IEEE Transactions on Power Delivery, April., 2021.